molecular pharmaceutics

articles

Preparation and in Vitro Evaluation of Topical Formulations Based on Polystyrene-poly-2-hydroxyl Methacrylate Nanoparticles

Xiao Wu,[†] Peter Griffin,[‡] Gareth J. Price,[‡] and Richard H. Guy*,[†]

Department of Pharmacy and Pharmacology, University of Bath, Claverton Down, Bath, BA2 7AY, U.K., and Department of Chemistry, University of Bath, Claverton Down, Bath, BA2 7AY, U.K.

Received April 29, 2009; Revised Manuscript Received July 16, 2009; Accepted July 24, 2009

Abstract: The skin disposition of topically applied nanoparticles with varying degrees of hydrophobicity, composed of different proportions of polystyrene (PS) and poly-(2-hydroxyethyl methacrylate) (HEMA), and of an associated, model "active" (Nile Red), was investigated. PS-HEMA copolymer nanoparticles were fluorescently labeled, via the covalent incorporation of a small quantity of fluorescein methacrylate, and characterized by dynamic light scattering, transmission electron microscopy and NMR. The fluorophore, Nile Red, was dispersed into the nanoparticles and its loading was determined by ultracentrifugation. Skin uptake was assessed in vitro following a 6 h application of the nanoparticle formulation, via stratum corneum (SC) tape-stripping and confocal microscopy. Nanoparticle diameters were below 100 nm. Progressive introduction of HEMA decreased particle hydrophobicity and reduced Nile Red loading. Uptake of Nile Red into the skin, as assessed both by the amounts extracted from the SC and by confocal microscopy, decreased as the percentage HEMA increased. Confocal microscopy confirmed that nanoparticles could not move beyond the superficial SC, but did show affinity for hair follicle openings. In conclusion, the loading of a lipophilic "active" into nanoparticles, and its subsequent release when these formulations are applied topically, are sensitive to the composition and relative hydrophobicity of the carrier.

Keywords: Nanoparticles; skin; laser scanning confocal microscopy (LSCM); tape-stripping

Introduction

The stratum corneum is the thin ($\sim$15 μm) outermost layer of the skin. It has been described as a "brick and mortar" structure (Wertz and Downing 1989) in which corneocytes are embedded in an intercellular lipid matrix. The corneocytes are arranged in parallel, overlapping, multicellular stacks perpendicular to the skin surface. The excellent permeability barrier of the skin protects the body against the loss of endogenous substances and from environmental insult.[1]

Nanoparticles (NP) incorporating drug or active ingredients have been employed in pharmaceutical and cosmetic formulations to increase transport into/across the skin, to improve the homogeneity of the vehicle's distribution on the skin, and to modulate flexibly the release of the active to the surface.[2−8] This has proved useful, for example, for those vehicles which are able to form thin, occlusive films that

* To whom correspondence should be addressed. Mailing address: Department of Pharmacy and Pharmacology, University of Bath, Claverton Down, Bath, BA2 7AY, U.K. Phone: +44.1225.384901. Fax: +44.1225.386114. E-mail: r.h.guy@bath.ac.uk.

[†] Department of Pharmacy and Pharmacology.

[‡] Department of Chemistry.

(1) Bouwstra, J. A.; Honeywell-Nguyen, P. L.; Gooris, G. S.; Ponec, M. Structure of the Skin Barrier and Its Modulation by Vesicular Formulations. *Prog. Lipid Res.* **2003**, *42*, 1–36.

(2) Alvarez-Roman, R.; Barre, G.; Guy, R. H.; Fessi, H. Biodegradable Polymer Nanocapsules Containing a Sunscreen Agent: Preparation and Photoprotection. *Eur. J. Pharm. Biopharm.* **2001**, *52*, 191–195.

(3) Lboutounne, H.; Chaulet, J. F.; Ploton, C.; Falson, F.; Pirot, F. Sustained Ex Vivo Skin Antiseptic Activity of Chlorhexidine in Poly(ε-Caprolactone) Nanocapsule Encapsulated Form and as a Digluconate. *J. Controlled Release* **2002**, *82*, 319–334.

10.1021/mp900119u CCC: $40.75
Published on Web 07/24/2009

Chart 1. The Chemical Structures of Polystyrene (PS), Fluorescein Methacrylate (FMA) and 2-Hydroxyethyl Methacrylate (HEMA)

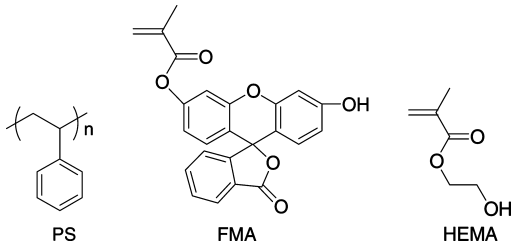

retain photoprotective actives. Increasingly, the physicochemical properties of the nanoparticles (size, charge, etc.) that determine their behavior once applied to the skin, and the kinetics with which an "active" is released, are being understood (ref 9 and the present article's companion paper, DOI 10.1021/mp9001188[10]), and have formed the basis of earlier research upon which the present study builds.

Here, four polystyrene (PS)-2-hydroxyethyl methacrylate (HEMA) NP dispersions were prepared and tested on porcine skin. The influence of polymer hydrophobicity on the skin uptake of Nile Red (NR), a model "active" compound was investigated. As reported previously in the companion paper (DOI 10.1021/mp9001188[10]), a small amount of fluorescein methacrylate (FMA) was introduced into the polymerization process to covalently label the nanoparticles and permit their disposition on and within the skin to be monitored as well. The structures of PS, FMA and HEMA are in Chart 1.

Materials and Methods

Tissue. Full thickness porcine skin was obtained from a local slaughterhouse. The skin was cleaned carefully under cold running water. The subcutaneous fat was removed with a scalpel. The remaining tissue was dermatomed to a thickness of ~750 μm. Finally, the dermatomed skin was stored frozen at −20 °C for up to a maximum of one month before use. Porcine skin has been widely used as a substitute for human skin in studies of topical/transdermal drug delivery. Porcine and human skins have remarkable similarities in epidermal thickness, lipid composition and permeability to diverse compounds.[11−14] Other biophysical properties, such as transepidermal water loss and low-frequency impedance, also show a remarkable overlap with those of the human counterpart.[15] The effect of storage duration on skin used for in vitro experiments has been carefully examined,[13] and there has been no significant effect observed on barrier function for periods much longer than those employed in this work.

Chemicals. Fluorescein *O*-methacrylate (FMA, 97% pure), Nile Red (NR, analytical grade) and polystyrene (MW = 44,000) were purchased from Sigma-Aldrich (St. Louis, MO). Styrene (99% GC), 2-hydroxyethyl methacrylate (HEMA, 98%), potassium persulfate (KPS) and dichloromethane (HPLC grade) were purchased from Sigma-Aldrich (Gillingham, Dorset, England). Other chemicals used were sodium dodecylsulfate (SDS, 99+% GC, Sigma-Aldrich, Japan), ruthenium tetroxide (Taab Laboratories, Aldermaston, England), and chloroform-d_1 (ISOTEC TM, Miamisburg, OH).

NP Preparation. Styrene was first purified by passage through an alumina column to remove inhibitors. Nanoparticles were then prepared in an inert nitrogen atmosphere by free radical polymerization (Scheme 1). Fluorescein methacrylate (FMA, 0.13 g) and Nile Red (NR, 0.01 g) were dissolved in 13 g of a mixture of styrene and 2-hydroxyethyl methacrylate (HEMA) and deoxygenated under N_2. Four distinct compositions of the monomers were used containing, respectively, 0, 5, 10 and 20% w/w HEMA. Sodium dodecylsulfate (SDS, 1 g), an emulsifier, and potassium persulfate (KPS, 0.1 g), a free radical initiator, were dissolved in 200 mL of distilled water in a round-bottomed flask and degassed under N_2. This solution was then heated to ~75 °C before the oil phase was added with vigorous stirring. Polymerization and NP formation was carried out for 3 h.

(4) Miyazaki, S.; Takahashi, A.; Kubo, W.; Bachynsky, J.; Loebenberg, R. Poly N-Butylcyanoacrylate (PNBCA) Nanocapsules as a Carrier for NSAIDs: In Vitro Release and in Vivo Skin Penetration. *J. Pharm. Pharm. Sci.* **2003**, *6*, 238–245.

(5) Luppi, B.; Cerchiara, T.; Bigucci, F.; Basile, R.; Zecchi, V. Polymeric Nanoparticles Composed of Fatty Acids and Polyvinylalcohol for Topical Application of Sunscreens. *J. Pharm. Pharmacol.* **2004**, *56*, 407–411.

(6) Shim, J.; Seok Kang, H.; Park, W. S.; Han, S. H.; Kim, J.; Chang, I. S. Transdermal Delivery of Minoxidil with Block Copolymer Nanoparticles. *J. Controlled Release* **2004**, *97*, 477–484.

(7) Luengo, J.; Weiss, B.; Schneider, M.; Ehlers, A.; Stracke, F.; Konig, K.; Kostka, K. H.; Lehr, C. M.; Schaefer, U. F. Influence of Nanoencapsulation on Human Skin Transport of Flufenamic Acid. *Skin Pharmacol. Physiol.* **2006**, *19*, 190–197.

(8) Kaur, I. P.; Agrawal, R. Nanotechnology: A New Paradigm in Cosmeceuticals. *Recent Pat. Drug Delivery Formulation* **2007**, *1*, 171–182.

(9) Wu, X.; Biatry, B.; Cazeneuve, C.; Guy, R. H. Drug Delivery to the Skin from Sub-micron Polymeric Particle Formulations: Influence of Particle Size and Polymer Hydrophobicity. *Pharm. Res.* **2009**, *26*, 1995–2001.

(10) Wu, X.; Price, G. J.; Guy, R. H. Disposition of Nanoparticles and an Associated Lipophilic Permeant following Topical Application to the Skin. *Mol. Pharmaceutics*. DOI: 10.1021/mp9001188.

(11) Sekkat, N.; Guy, R. H. Biological Models to Study Skin Penetration. In *Pharmacokinetic Optimization in Drug Research*; Testa, B., van de Waterbeemd, H., Folkers, G. , Guy, R. H. , Eds.; Wiley-VCH: Weinheim, Germany, 2001; pp 155−172.

(12) Wertz, P. W.; Downing, D. T. Stratum Corneum: Biological and Biochemical Considerations. In *Transdermal Drug Delivery*, 1st ed.; Hadgraft, J., Guy, R. H., Eds.; Marcel Dekker, Inc.: New York, 1989; pp 1−22.

(13) Williams, A. C. *Transdermal and Topical Drug Delivery*; Pharmaceutical Press: London, 2003; pp 51−82.

(14) Herkenne, C.; Naik, A.; Kalia, Y. N.; Hadgraft, J.; Guy, R. H. Pig Ear Skin ex vivo as a Model for in vivo Dermatopharmacokinetic Studies in Man. *Pharm. Res.* **2006**, *23*, 1850–1856.

(15) Sekkat, N.; Kalia, Y. N.; Guy, R. H. Biophysical Study of Porcine Ear Skin in Vitro and Its Comparison to Human Skin in Vivo. *J. Pharm. Sci.* **2002**, *91*, 2376–2381.

Scheme 1. Preparation of Styrene-2-hydroxyethyl Methacrylate (HEMA)-fluorescein Methacrylate (FMA) Copolymers by Emulsion Radical Copolymerization with Potassium Persulfate (KPS) at 75°C

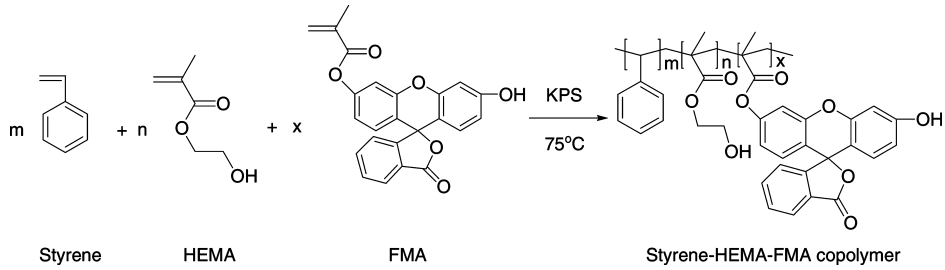

The resulting particles contained FMA covalently and randomly incorporated into the PS-HEMA polymer. NR was absorbed on/in the NP.

NP Characterization. The mean size and polydispersity of the NP were measured by dynamic light scattering (DLS) (BI90Plus spectrophotometer, Brookhaven Instruments Corporation, NY). NP morphology was observed on a JEOL (JEM-2000) transmission electron microscope (TEM) at an accelerating voltage of 120 kV. Each sample was prepared by casting a drop of NP dispersion onto a 300-mesh copper grid covered with carbon film. TEM images of the NP were obtained as positively stained preparations by placing samples in ruthenium tetroxide vapor for 1 h.[16]

To determine the degree of Nile Red incorporation into the nanoparticles, the formulations were filtered (0.45 μm nylon filters, Whatman, Japan) and then subjected to ultracentrifugation at 17000*g* for 3 h at 20 °C. The supernatant was kept for analysis of Nile Red. The sediment was washed with distilled water to remove surfactant and again centrifuged at 17000 g for 3 h. The resulting pellet was freeze-dried, and then dissolved in dichloromethane. Finally, Nile Red in this organic solvent was measured by HPLC (Dionex, Sunnyvale, CA) with fluorescence detection at 559 and 630 nm for excitation and emission wavelengths, respectively. A Hypersil BDS C18 (5 μm) 250 × 4.6 mm column was used, and the mobile phase was dichloromethane pumped at a flow rate of 1 mL/min at 25 °C. Each injection was 200 μL. The Nile Red retention time was 5.6 min. Nile Red in the supernatant was also measured by HPLC using a mobile phase comprising acetonitrile−water (80:20). The column, injection volume, and temperature were as above. The retention time in this case was 12.1 min.

^{1}H NMR spectra were recorded in deuterated chloroform ($CDCl_3$) on a Bruker Avance III spectrometer (Billerica, MA) operating at 400 MHz. Prior to analysis in $CDCl_3$, the NP were washed with water and acetone to remove SDS and unreacted compounds, and freeze-dried (Heto PowerDry PL3000, Thermo Electron Corporation, Waltham, MA).

In Vitro Skin Permeation. Following NP preparation as described above, the dispersions were filtered to remove insoluble and nonincorporated NR, and then subjected to ultracentrifugation at 17000*g* for 3 h at 20 °C. The sediment was washed with distilled water to remove surfactant and redispersed in water.

Visible hairs on the skin were first trimmed as close as possible to the surface. Skin permeation experiments were performed in vertical Franz diffusion cells thermostated at 37 °C. The excised tissue was clamped between the donor and receptor compartments exposing a diffusion area of 3.8 cm^2. The receptor phase was physiological buffer (pH = 7.4); the donor compartment held 1 mL of the NP formulation and was covered with Parafilm. After an application lasting 6 h, the cell was dismantled, and the skin was immediately either examined by confocal microscopy or tape-stripped to determine the NR concentration profile across the SC.

Laser Scanning Confocal Microscopy (LSCM). The treated skin was first cleaned with physiological buffer and dried with tissue. Physiological buffer (~5 mL) was introduced into a small culture plate. Treated skin was immersed in the buffer and agitated gently for 1 min. The process was repeated three times. As the NP formulation was aqueous-based, any material remaining on the surface was readily removed in this way. The skin surface was gently patted dry by the repeated application of absorbent tissues.

The skin was then examined using a LSM 510 Invert Laser Scanning Microscope (Carl Zeiss, Jena, Germany). The system was equipped with both an argon laser (excitation line at 488 nm) and a HeNe laser (excitation line at 543 nm). A Plan-Neofluar 10×/0.3 objective, an EC Plan-Neofluar 40×/1.30 oil DIC M27 objective and a Plan-Apochromat 63×/1.40 oil DIC M27 objective were used. Confocal images were obtained in the plane parallel to the sample surface (*xy*-mode), or in the plane perpendicular (optical sectioning *z*-stack mode).

Tape-Stripping. A validated tape-stripping procedure was used to assess the depth of NR penetration into the SC and to recover NR from the treated skin.[17−20] About twenty 2.7 × 2.7 cm^2 tapes were prepared (Scotch No. 845 Book Tape,

(16) Trent, J. S.; Scheinbeim, J. I.; Couchman, P. R. Ruthenium Tetraoxide Staining of Polymers for Electron Microscopy. *Macromolecules* **1983**, *16*, 589–598.

(17) Kalia, Y. N.; Alberti, I.; Sekkat, N.; Curdy, C.; Naik, A.; Guy, R. H. Normalization of Stratum Corneum Barrier Function and Transepidermal Water Loss In Vivo. *Pharm. Res.* **2000**, *17*, 1148–1150.

(18) Herkenne, C.; Naik, A.; Kalia, Y. N.; Hadgraft, J.; Guy, R. H. Dermatopharmacokinetic Prediction of Topical Drug Bioavailability in vivo. *J. Invest. Dermatol.* **2007**, 887–894.

(19) Herkenne, C.; Naik, A.; Kalia, Y. N.; Hadgraft, J.; Guy, R. H. Effect of Propylene Glycol on Ibuprofen Absorption into Human Skin in vivo. *J. Pharm. Sci.* **2008**, *97*, 185–197.

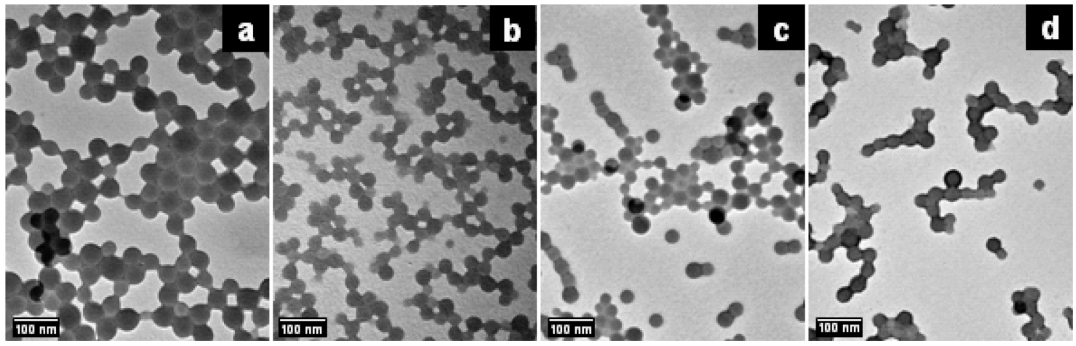

Figure 1. Transmission electron microscopy of nanoparticles stained with ruthenium tetroxide: (a) PS; (b) PS-HEMA (95/5); (c) PS-HEMA (90/10); (d) PS-HEMA (80/20). Scale bar = 100 nm.

3M Media, Broken, Germany). To delimit a fixed area for tape stripping, a 5 × 5 cm square mask was prepared with a central aperture of 2 cm diameter. A strip of adhesive tape was pressed firmly onto the skin surface, and then removed in a single movement. The direction of stripping was changed with each tape to ensure a more uniform removal of the SC with fewer tape-strips. Before and after each tape-strip, transepidermal water loss (TEWL) across the skin was measured (Aquaflux, Biox Systems Ltd., London, U.K.) to provide an idea of when most of the SC had been removed and to signal the end of the tape-stripping process. This was considered appropriate when TEWL reached 80 $g^{-1}\cdot m^{-2}\cdot h$.[20] The tapes were weighed before and after stripping to determine the mass of SC removed. As the density of the tissue is ~1 g/cm^3[3,21] the volume of SC removed by each strip is known (assuming uniform coverage of SC on the tape-strip).[22] Then, given that the area stripped is fixed, the thickness of SC removed as tape-stripping proceeds can be found.

Results and Discussion

For each polymerization, the measured conversions were >90%. The NP were spherical and smooth, as shown by TEM (Figure 1). The mean diameter of the NP was less than 100 nm, an observation confirmed by dynamic light scattering (DLS) (Table 1).

NR encapsulation varies inversely with the percentage of HEMA copolymerized into the nanoparticles (Table 1). That is, as the hydrophobicity of the particles was reduced (by increasing the amount of HEMA relative to PS), the affinity of the lipophilic dye, Nile Red, for the polymer decreased proportionally. A relatively constant amount of Nile Red was recovered in the supernatant for all nanoparticles, and it is inferred that the remaining fraction of the dye was associated with surfactant micelles.

Table 1. Properties of the Nanoparticle Formulations Considered

nanoparticle formulation	av diameter (nm)	PI[a]	% Nile Red[b]	
			associated	in supernatant
polystyrene (PS)	73.8	0.092	73.15 ± 1.14	6.43 ± 0.48
PS-5% HEMA	45.8	0.12	59.42 ± 2.07	6.21 ± 0.35
PS-10% HEMA	43.2	0.13	41.06 ± 1.85	6.20 ± 0.33
PS-20% HEMA	36.7	0.165	17.66 ± 1.20	6.20 ± 0.35

[a] PI: polydispersity index of the size distribution (expressed using a 0−1 scale). [b] Mean ± SD, $n = 5$.

Proton NMR spectra of HEMA, polystyrene, and the copolymer are shown in Figure 2. The copolymer shows signals from polystyrene and HEMA even after extensive dissolution/reprecipitation. However, because of the polymerization reaction, the copolymers do not have signals at 5.6 and 6.1 ppm, which are present in HEMA's spectrum. While we did not investigate the polymer microstructure in detail, the spectra revealed no evidence of formation of blocks of the two monomers.

Laser Scanning Confocal Microscopy. The dual-fluorescently labeled nanoparticles permitted the simultaneous visualization of the disposition/penetration of the carriers and of the model active (Nile Red) on and within the superficial skin. Moreover, the treated skin could be mechanically cross-sectioned as well, enabling the distribution of the fluorescent probes to be visualized as a function of depth. In this case, the confocality of the microscope used permitted artifacts from the sectioning to be avoided.[23−25]

Figure 3 shows LSCM images of skin treated with PS nanoparticles. Localization and release of Nile Red in skin "furrows" is apparent in the images from the skin surface.

(20) N'Dri-Stempfer, B.; Navidi, W. C.; Guy, R. H.; Bunge, A. L. Improved Bioequivalence Assessment of Topical Dermatological Drug Products Using Dermatopharmacokinetics. *Pharm. Res.* **2009**, *26*, 316–328.

(21) Anderson, R. L.; Cassidy, J. M. Variation in Physical Dimensions and Chemical Composition of Human Stratum Corneum. *J. Invest. Dermatol.* **1973**, *61*, 30–32.

(22) Kalia, Y. N.; Pirot, F.; Guy, R. H. Homogeneous Transport in a Heterogeneous Membrane: Water Diffusion across Human Stratum Corneum in Vivo. *Biophys. J.* **1996**, *71*, 2692–2700.

(23) Shotton, D. M. Confocal Scanning Optical Microscopy and Its Application for Biological Specimens. *J. Cell Sci.* **1989**, *94*, 175–206.

(24) Alvarez-Roman, R.; Naik, A.; Kalia, Y. N.; Fessi, H.; Guy, R. H. Visualization of Skin Penetration Using Confocal Laser Scanning Microscopy. *Eur. J. Pharm. Biopharm.* **2004**, *58*, 301–316.

(25) Alvarez-Roman, R.; Naik, A.; Kalia, Y. N.; Guy, R. H.; Fessi, H. Skin Penetration and Distribution of Polymeric Nanoparticles. *J. Controlled Release* **2004**, *99*, 53–62.

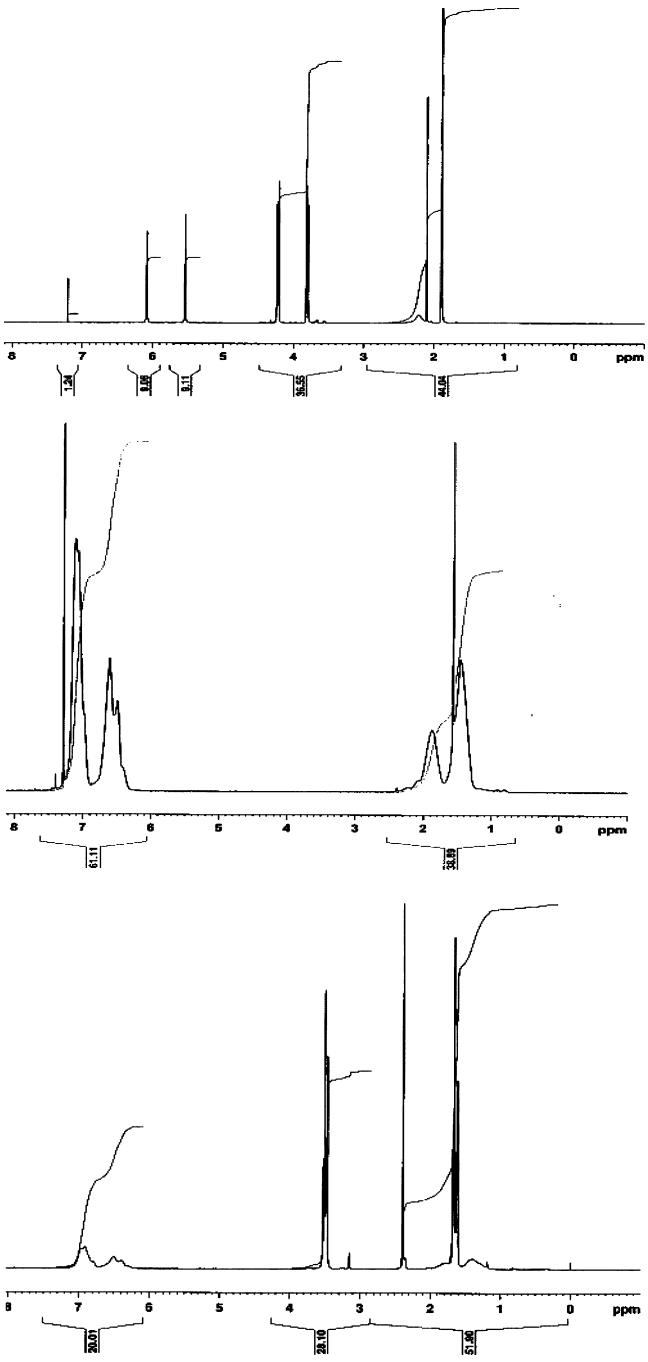

Figure 2. ^{1}H NMR spectra of HEMA (top), polystyrene (middle) and their copolymer (bottom).

However, the green fluorescence from the polymer itself is very weak, suggesting that the cleaning procedure efficiently removed the particles post-treatment. The cross-sectional images confirm these observations and show that Nile Red is released and penetrates into the deeper SC, in agreement with the results from previous studies.[24−26] The overlay images of green and red fluorescence reveal only the presence of the latter.

(26) Bouwstra, J. A.; Dubbelaar, F. E. R.; Gooris, G. S.; Ponec, M. The Lipid Organisation in the Skin Barrier. *Acta Derm.-Venereol., Suppl.* **2000**, *208*, 23–30.

The behavior of PS nanoparticles containing 5% HEMA is shown in Figure 4. It is apparent that less Nile Red uptake into the SC has taken place. Once again, the persistence of the particles themselves post-treatment and surface cleaning is poor although there is evidence in Figure 4d that the carriers have been noticeably retained on a hair stub, and that the Nile Red has remained largely associated with the polymer here. Again, this observation is consistent with earlier reports in the literature.[24,25]

Figure 5 continues the trend seen in Figure 4 and illustrates the disposition of PS nanoparticles with 10% HEMA. Affinity of the particles for follicular structures is clearly observed, with the Nile Red colocalized with the polymer. On the skin surface, in contrast, the model active has separated from the carrier.

Finally, when the HEMA content in the PS nanoparticles is raised to 20%, the images post-treatment and surface cleaning reveal only very faint red fluorescence, with no sign of retained polymer as shown in Figure 6. In this case, the Nile Red loading is very low, such that the driving force for permeation (even supposing an efficient release from the nanoparticle) is low. Overall, the confocal experiments reveal that (i) introducing hydrophilicity into the nanoparticles alters their behavior on skin; (ii) the disposition of an associated lipophilic "active" (Nile Red) is influenced by nanoparticle properties; (iii) increasing the percentage of HEMA in PS nanoparticles significantly reduces the uptake of Nile Red into the SC; and (iv) there is no evidence that nanoparticles can penetrate beyond superficial SC. The latter conclusion agrees completely with recent findings from multiphoton microscopy experiments tracking the fate of poly(lactide-*co*-glycolide) nanoparticles in the SC.[27]

In Vitro Skin Penetration. In all experiments, irrespective of the nanoparticle composition used, no fluorescence (red or green) was ever detected in the receptor phase, confirming the LSCM observations that the disposition of the various formulation compounds was constrained to the SC.

The SC concentration profiles of Nile Red delivered from the four different nanoparticle carriers are in Figure 7. From the concomitant measurements of TEWL and of the mass of SC removed on each tape, it was possible (as previously published[17−19,22]) to express the concentrations as a function of relative position within the SC, thereby correcting for differences in absolute SC thickness from one porcine skin sample to another. This approach is reflected in the good reproducibility in the obtained results, and the clear separation, in terms of Nile Red uptake, between the nanoparticle formulations.

As the NR concentration (C_{veh}) in each formulation was known (Table 1), the SC concentration (C_x) versus normalized depth (x/L) profiles of NR in Figure 7 were fitted to the appropriate solution of Fick's second law of diffusion (eq 1):

$$C_x = K \cdot C_{veh}\{1 - \frac{x}{L} - \frac{2}{\pi}\sum_{n=1}^{\infty}\frac{1}{n}\cdot\sin(n\pi\frac{x}{L})\cdot\exp(-\frac{D}{L^2}\cdot n^2\pi^2 t)\} \quad (1)$$

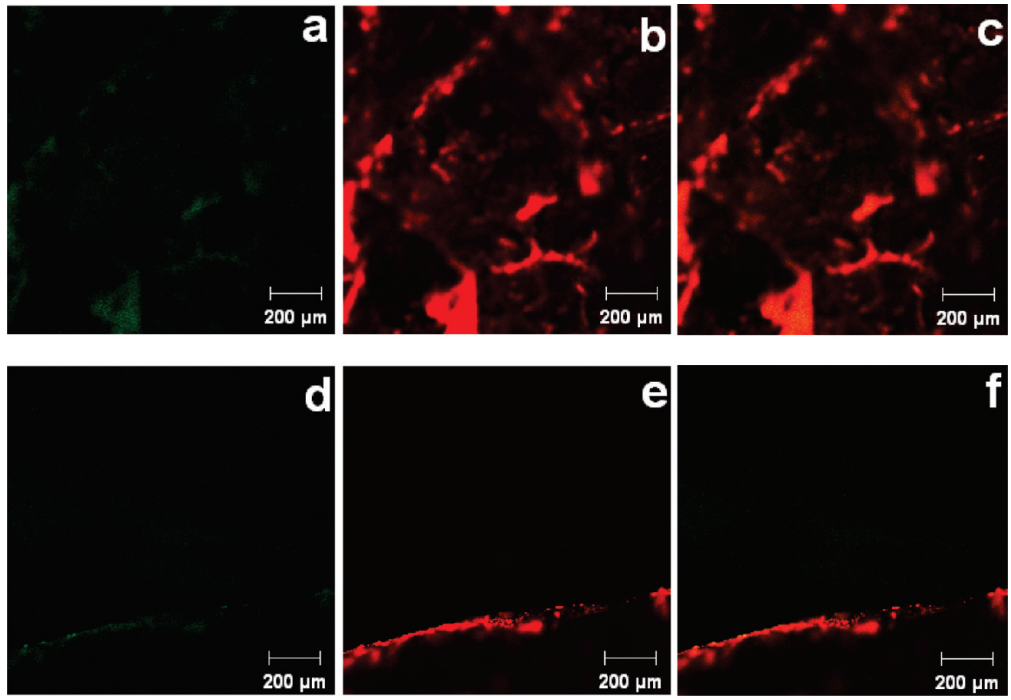

Figure 3. PS nanoparticle-treated skin surface (top) and cross-sectional images (below). (a, d) Green fluorescence from the FMA, indicating the location of the polymer. (b, e) Red fluorescence from Nile Red. (c, f) Overlaid images of green and red fluorescence.

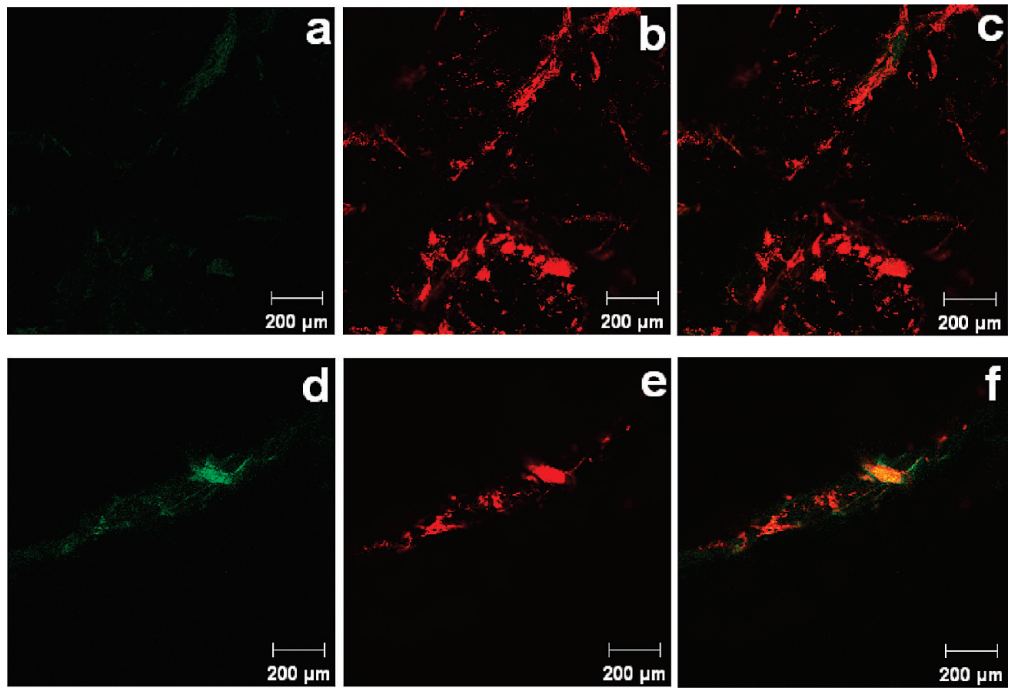

Figure 4. PS-5% HEMA nanoparticle-treated skin surface (top) and cross section images (below). (a, d) Green fluorescence from the FMA, indicating the location of the polymer. (b, e) Red fluorescence from Nile Red. (c, f) Overlaid images of green and red fluorescence.

This equation assumes that (i) the applied NR concentration remains constant for the treatment period (t); (ii) the viable epidermis is a perfect sink for the permeant; (iii) the SC contains no NR at $t = 0$. The fitting procedure yielded the SC/vehicle partition coefficient (K) of NR and its characteristic diffusion parameter (D/L^2, where D is NR's diffusivity across the SC of thickness L). The quantitative parameters are shown in Table 2. The values of K for NR partitioning from PS, PS-5% HEMA and PS-10% HEMA polymers into the SC are reasonably constant. When the HEMA content

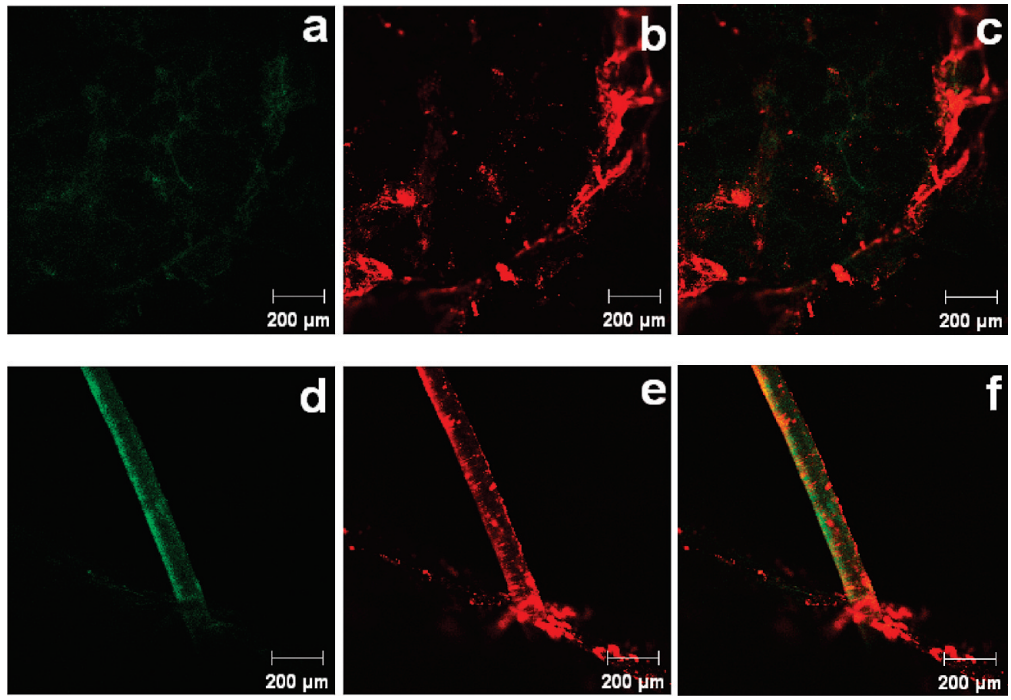

Figure 5. PS-10% HEMA nanoparticle-treated skin surface (top) and cross section images (below). (a, d) Green fluorescence from the FMA, indicating the location of the polymer. (b, e) Red fluorescence from Nile Red. (c, f) Overlaid images of green and red fluorescence.

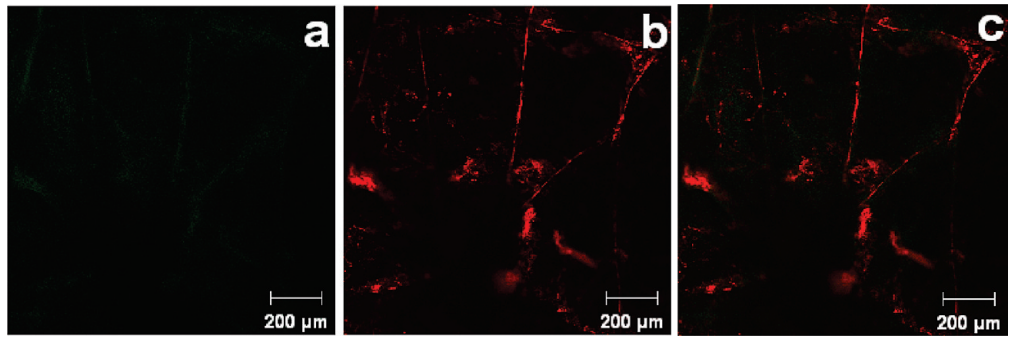

Figure 6. PS-20% HEMA nanoparticle-treated skin surface (top). (a) Green fluorescence from the FMA, indicating the location of the polymer. (b) Red fluorescence from NR. (c) Overlaid image of green and red fluorescence. Red fluorescence was not observed in cross section skin samples, due to inefficient Nile Red penetration in the SC.

was 20%, a decrease in K was apparent. As expected, the values of D/L^2 for NR diffusion into the SC were similar between the nanoparticle formulations.

The accumulated amount of NR taken up from each PS-HEMA polymer at the end of the application period was determined by summing the quantities recovered from the individual tape-strips (Figure 8). These results reinforce the fact that Nile Red penetration into the SC was significantly reduced with each increment in the percentage HEMA incorporated into the polymer. The diminishing load of Nile Red in the nanoparticles as the percentage HEMA was increased (Table 1) almost certainly underlies the trend in

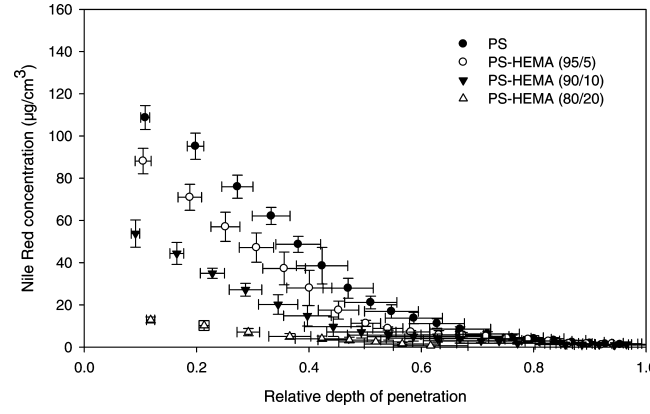

Figure 7. Concentration profiles of Nile Red across the SC as a function of relative depth into the membrane (n = 5, mean ± SD), where 0 indicates the SC surface and 1 reflects the SC−stratum granulosum interface.

(27) Stracke, F.; Weiss, B.; Lehr, C. M.; Konig, K.; Schaefer, U. F.; Schneider, M. Multiphoton Microscopy for the Investigation of Dermal Penetration of Nanoparticle-Borne Drugs. *J. Invest. Dermatol.* **2006**, *126*, 2224–2233.

Table 2. Values of K and D/L^2 of NR in the SC (Mean ± SD, $n = 5$) following a 6 h Application of Polystyrene-HEMA Nanoparticle Formulations

PS-HEMA nanoparticles (HEMA %)	K[a]	D/L^2 (h^{-1})[b]
0	3653 ± 165	0.011 ± 0.002
5	3516 ± 200	0.009 ± 0.001
10	2998 ± 345	0.008 ± 0.001
20	1662 ± 256	0.009 ± 0.003

[a] Partition coefficient estimated by fitting the permeation data to eq *1*. [b] Diffusion coefficient divided by the diffusion length squared estimated by fitting the permeation data to eq *1*.

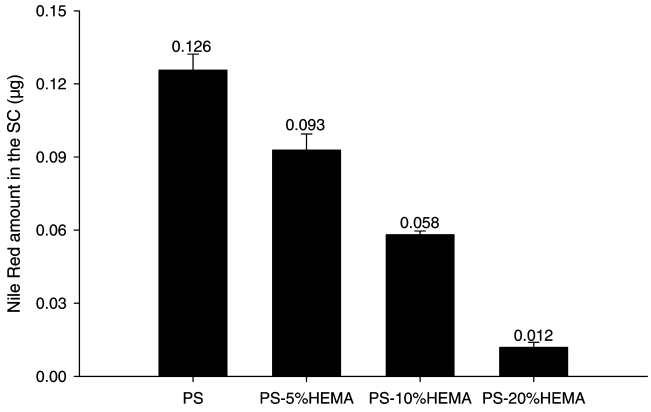

Figure 8. Total quantities (in μg) of Nile Red in the SC after a 6 h application of four NP formulations ($n = 5$, mean ± SD). A one-way ANOVA followed by Tukey's multiple comparison test shows that each amount of NR uptake into the SC differed significantly from all of the others ($P < 0.001$).

Figure 8. Indeed, if the average amounts of the dye taken up into the SC are divided by the fraction of the active eventually associated with the particles, the ratios are remarkably consistent: 0.17, 0.16, 0.15, and 0.07 for PS, PS-5% HEMA, PS-10% HEMA and PS-20% HEMA, respectively. The apparent divergence for the nanoparticles containing the greatest level of HEMA is probably due, at least in part, to the fact that detection of Nile Red in many of the SC tape-strips following treatment with this formulation was close to or below the limits of quantitation/detection.

It is appropriate to point out that these findings concur with earlier work from our laboratory in which the SC uptake of Nile Red was observed to decrease as the nanoparticle polymer was changed from PS to poly caprolactone to cellulose acetate butyrate; in other words, as the polymer became progressively more hydrophilic.[9] As has been seen here, despite employing the same amount of Nile Red in the nanoparticle preparation procedure, the quantity eventually associated with the carrier depends upon polymer properties, and becomes less and less as the hydrophilicity is increased.

Conclusions

The incorporation of a lipophilic active (Nile Red) into a series of PS nanoparticles was sensitive to the percentage of the hydrophilic copolymer (HEMA) present. As a result, the uptake of the active into the skin, following topical application of the nanoparticle formulations, was less efficient as the hydrophobicity of the carriers decreased. Results from confocal microscopy and SC tape-stripping experiments underpin these conclusions and provide valuable tools, therefore, for the development and optimisation of future nanoparticle formulations.

Abbreviations Used

DLS, dynamic light scattering; FMA, fluorescein methacrylate; HEMA, poly-2-hydroxyethyl methacrylate; KPS, potassium persulfate; LSCM, laser scanning confocal microscope; NMR, nuclear magnetic resonance; NP, nanoparticle(s); NR, Nile Red; PI, polydispersity index; PS, polystyrene; SC, stratum corneum; SDS, sodium dodecylsulfate; TEM, transmission electron microscope; TEWL, transepidermal water loss.

Acknowledgment. Supported by the European Commission 6th Research and Technological Development Framework Programme (NAPOLEON: Nanostructured Waterborne Polymer Films with Outstanding Properties) and a University Research Scholarship for X.W.

MP900119U